Improved magnetic particle tracking technique in dense gas fluidized beds

K.A.Buist[1], A.C. van der Gaag[1], N.G. Deen[1,*], and J.A.M. Kuipers[1]

[1]*Multiphase Reactors group, Department of Chemical Engineering & Chemistry, Eindhoven University*

of Technology, P.O. box 513, 5600 MB Eindhoven, The Netherlands

[*]*Corresponding author, E-mail: N.G.Deen@tue.nl*

Abstract

Non-invasive monitoring of multiphase flow is rapidly gaining increased interest. More specifically non-invasive particle tracking techniques have received a lot of attention in recent years to study dense granular flow. However, these techniques are usually quite expensive and require strict safety measures. In this paper an improved magnetic particle tracking (MPT) technique for dense granular flow will be presented. The improvements of the analysis technique for MPT will be demonstrated and rigorously tested with a 3D system and 2D sensor system. The strengths and limitations of the MPT technique will also be reported. Finally the results of the MPT are compared with data obtained from a combined particle image velocimetry (PIV) and digital image analysis (DIA) technique.

Introduction

Gas solid fluidization is an important industrial multiphase operation for various chemical and physical processes in the industry, including gasification, combustion, catalytic cracking, gas phase polymerization, drying and coating. Favourable characteristics include excellent solids mixing, good contacting between gas and solids and excellent heat transfer characteristics. Because these multiphase flows are highly complex, they have been subject to many studies, both experimentally and computationally. Recent advances in computational power and modelling have allowed detailed studies of solids motion, gas back mixing and gas-solid interactions. This consequently asks for more and/or better experimental methods for validation. The outcome of these studies should eventually lead to improvements in operation and design.

Most of the experimental techniques used in dense granular flows rely on non-invasive monitoring techniques. Among these, particle tracking techniques have shown great potential in characterization of dense granular flows: mixers, fluidized- and spouted beds. Positron Emission Particle Tracking (PEPT)[1], Radioactive Particle Tracking (RPT), computer aided radioactive particle tracking (CARPT)[2] and Particle Tracking Velocimetry (PTV) are the most well known[3]. Recently a new and promising technique was introduced; Magnetic Particle Tracking (MPT). MPT is a technique that has been used in the medical field to study the motility tract and targeted drug delivery[4] and originates from the work of Richert et al.[5]. Typically this technique uses a small magnetic source, usually a magnetic dipole, the magnetic signal of which can be detected by a series of sensors. Based on these signals a reconstruction of the magnetic field can be made and thus the position and orientation of the magnet can be determined via an appropriate algorithm.

One of the main advantages of the MPT over other particle tracking techniques is its relative low cost and the ease of use with respect to PEPT or RPT and its compatibility with 3D systems with respect to PTV. In PEPT and RPT the sensors and the use,

2

preparation and handling of radioactive tracer material introduces high cost and special safety issues. In MPT the use of tri-axis Anisotropic Magneto Resistive (AMR) sensors and neodymium magnets reduces the costs by at least a factor 10 and has no safety issues. MPT, however, is restricted by the use of rather large magnetic markers, a topic which will be addressed in this work. The magnetic field strength sensed at the sensor does not only depend on the strength of the magnet and the distance to the sensors, but also on the relative orientation of the magnet to the sensor. This allows to also study rotational motion, which might be especially interesting for non-spherical particles. Table 1 summarizes the advantages and disadvantages of several particle tracking techniques.

The use of MPT in dense granular flow has first been proposed by Mohs et al.[6] in a spout fluidized bed. They were able to follow a rather large magnetic marker at 62.5 Hz. Halow et al.[7] studied segregation effects in fluidized beds using just four Hall effect sensors. Finally Neuwirth et al.[8] have used MPT to enable comparison of measured particle motion in a rotor granulator with simulated results obtained from Discrete Element Model (DEM). An increase of the measurement rate to 200 Hz in their study revealed an increase in accuracy. Furthermore, Idakiev and Mörl[9] have recently used MPT to study particle trajectories and solids translation motion in a prismatic spouted bed and a fluidized bed.

For MPT to compete as a technique for particle tracking in granular flow, the limits of the technique have to be established and expanded. Also a first comparison with established techniques for granular flow is currently lacking. Hu et al.[10] have studied the effects of multiple non-linear optimization algorithms build for speed mostly. In this work we will present a new algorithm which is able to determine the position and orientation more accurately and more precise. The new MPT technique will be tested using a set of comprehensive tests and will finally be compared with a well-established technique; Particle Image Velocimetry combined with Digital Image Analysis[11,12] (PIV-DIA).

The organization of this paper is as follows. In section 2, the experimental setup will be described whereas in section 3 the principle of the two experimental techniques will

3

be discussed. In the fourth section, the new MPT analysis technique will be tested and finally in section 5, the results of the MPT and PIV-DIA techniques will be compared.

EXPERIMENTAL SETUP

For the MPT technique two sensor arrays are used. A pseudo 2D configuration to measure the particle motion for a pseudo 2D fluidized bed setup which is suitable to enable comparison with PIV-DIA. A 3D setup is used to test the limits of the experimental technique.

The 2D setup is presented in figure 1 and an overview of all settings and properties is given in table 2. The MPT sensor setup consists of an array of 6x4 tri-axis AMR-sensors, giving in total 72 signals. Setup and control are courtesy of Matesy GmbH, the setup is capable of measuring at 1000 Hz. The 2D sensor array is mounted to the frame of the pseudo 2D bed. A minimum distance of 0.02 m between the sensors and the domain of interest was maintained.

The pseudo 2D fluidized bed setup has dimensions of 0.3 x 0.015 x 1.0 m (W x D x H). The depth is chosen to be small enough to exhibit 2D behaviour and large enough to avoid bridging effects.The bottom is covered by a porous distributor plate of 3 mm thickness and an average pore size of 10 μm. All other parts of the setup are made of aluminium and non-magnetic stainless steel parts. The flow rate is controlled with a mass flow controller with a maximum capacity of 1200 l/min. The front plate is made of glass for visual access.

To be able to compare the MPT with the PIV-DIA technique the bed is illuminated using 4 LED-arrays for homogeneous illumination. Images are recorded using a LaVision HSG4M high speed camera with an image resolution of 2048 x 2048 pixels and images are captured at 200 Hz. Analysis of the images is done in Davis 8.1.7 and Matlab.

The 3D sensor array consists of 4 rings of 6 triaxis AMR sensors with a total height of 0.45 m and a distance of 0.26 m between opposing sensors. Figure 2 is a photo of the

4

3D sensor array, clearly depicting the 4 rings. Each ring contains 6 boxes with 3 sensors each, to a total of 72 sensors for the whole array. All the triaxis sensors are connected to a control box which reads the data and sends it to a lab computer. Before each experiment the offset of the sensors is determined, by measuring the field of an empty domain. After offset determination a magnetic marker can be added to the domain and the change in magnetic field can be measured.

PRINCIPLE

MAGNETIC PARTICLE TRACKING

The principle of the MPT measurement technique relies on tracking of a single magnetic marker. Evaluation of the quasi-static magnetic field results in a position estimate. This is an inverse problem with five degrees of freedom, three for position and two for orientation, (see figure 3). When the magnetic moment of the marker is unknown this can act as a sixth degree of freedom. The magnetic field is measured by several sensors that are positioned in a known configuration. The theoretical signals are calculated using the derivation of a magnetic field of a magnetic dipole at sufficient distance from the dipole:

$$\bar{H}(\bar{e}_p, \bar{r}_{ps}) = \frac{1}{4\pi} \left(-\frac{\mu_m \bar{e}_p}{|\bar{r}_{ps}|^3} + \frac{3\mu_m (\bar{e}_p \cdot \bar{r}_{ps})\bar{r}_{ps}}{|\bar{r}_{ps}|^5} \right) \tag{1}$$

With $\bar{r}_{ps} = \bar{r}_p - \bar{r}_s$, μ_m the magnetic moment of the marker , $\bar{e}_p$ the orientation unit vector of the magnet, calculated via a transformation of the angles; ϕ and θ from the spherical to the Cartesian coordinate system.

By multiplication of this magnetic field with the orientation of the sensor, the signal strength can be estimated:

$$S_t = \bar{H}(\bar{e}_p, \bar{r}_{ps}) \cdot \bar{e}_s \tag{2}$$

To determine the position and orientation, the theoretical signal strengths (S_t) given by equation 2 are compared to the actual signals given by the 72 sensors (S_m). The difference

5

between the two fields is minimized using a quality function:

$$Q = \sum_{i=1}^{72} \frac{((S_{m,i} - \langle S_m \rangle) - (S_{t,i} - \langle S_t \rangle))^2}{\Delta S_{m,i}^2} \tag{3}$$

The quality function 3 is corrected for deviations in each individual sensor given by a min/max deviation $(\frac{1}{\Delta S_{m,i}^2})$, this ensures that less accurate sensors, have less influence on the quality function. Secondly, the quality function is corrected for stray fields using a gradiometer $(\langle S \rangle)$.

Non-Linear Optimization

Hu et al.[10] have studied several optimization algorithms among which a linear function for the initial guess and several non-linear optimization methods to determine the optimum. They found the Levenberg-Marquardt (LM)[10] algorithm to be both fast and accurate. For research purposes the algorithm does not need to be fast and hence different optimization algorithms can be investigated. The effectiveness of the optimization algorithm can be improved by providing as much information from the experiment as possible. Besides the 72 sensor signals this also includes the bounds for the possible marker positions. Some non-linear optimization methods allow such constraints to the solution. In this work, the strength of the Sequential Quadratic Programming (SQP)[13] algorithm will be shown. For the pseudo 2D setup the following constraints have been set, slightly outside the physical domain to allow for error margins:

$$-0.2 \leq x \leq 0.2 \tag{4}$$
$$-0.3 \leq y \leq 0.3$$
$$0.01 \leq z \leq 0.07$$

6

For the 3D setup the following constraints have been set:

$$\sqrt{x^2 + y2} \leq 0.13 \tag{5}$$

$$0.3 \leq z \leq 0.3$$

In the LM-algorithm the solution of equation 1 is done by solving for the positions x, y, z and the angles φ, θ. Because φ is periodic, estimates across this periodic boundary, 180 to -180, are difficult to solve and result in erroneous solutions. The SQP algorithm allows for the addition of an extra degree of freedom by changing to the orientation unit vector and adding a non-linear constraint for the norm of the vector:

$$|\bar{e}_p| = 1 \tag{6}$$

$$-1 \leq e_x \leq 1$$

$$-1 \leq e_y \leq 1$$

$$-1 \leq e_z \leq 1$$

These three degrees of freedom are tied by one extra function, in effect reducing the total number of degrees of freedom back to five.

Signal filtering

In particle tracking techniques the sensor signals are often filtered to suppress high noise levels. Among those, wavelet filters are often used for their capability to handle sharp transitions in the signal[2]. Depending on the size of the magnet the signal on the sensors can be quite noisy and smart ways of filtering have to be used. The Levenberg-Marquardt method uses an averaging filter, which in principle reduces the measuring frequency from 1000 Hz to 50 or 200 Hz. We found that the use of a wavelet filter allows for smoother signal data and increases the accuracy of the optimization method. The wavelet toolbox of Matlab is used to separate noise from the signal. In principle any near symmetric

7

wavelet function would do.

Initialization

Gradient-search methods like the LM and SQP algorithms, need an initial estimate to converge to a local minimum of the target function 3. At the beginning of the analysis the algorithm is initialized using a multistart method, a functionality in Matlab. This multistart method uses multiple starting positions to find the global minimum. For any consecutive time step, the previous time step is used as an initial estimate. However, if the algorithm is unable to converge or the quality function is too high, the algorithm is set to reinitialize. Principally, if the algorithm finds its minimum on the boundary/constraint of the setup, this solution must be seen as erroneous and the algorithm is also set to reinitialize. Any final solution at the physical constraints is seen as an outlier.

Velocity and solids fraction

The velocity of the magnetic marker follows from the first order displacement vector:

$$\bar{v}_p(x,t) = \frac{\bar{r}_{ps(i+1)} - \bar{r}_{ps(i)}}{\Delta t}$$

From the position data the occupancy of the marker is determined via:

$$O(i,j) = \frac{N_{gridcells}}{N_{meas}} \sum_1^{N_{meas}} \delta \quad \forall p \left| \begin{array}{ll} \delta = 1 & p \in (i,j) \\ \delta = 0 & p \ni (i,j) \end{array} \right|$$

Meaning that the total counts of the marker in a certain cell is summed and normalized to the total counts. A value of 1 would mean an expected average value over the whole domain, higher values mean that the marker was in that part of the system more often than the rest of the domain. To compare the MPT with the DIA the occupancy is converted in a local solids fraction. This is done in a similar way as Wildman et al. [14]

8

using equation 7:

$$\varepsilon_s(i,j) = min\left(\frac{\frac{\pi d_p^3}{6}N_p}{V_{i,j}}\frac{O(i,j)}{N_{gridcells}}, 0.6\right) \qquad (7)$$

The maximum solids volume fraction is cut-off at 0.6, which is a common value for fluidized beds with Geldart B/D particles.

PARTICLE IMAGE VELOCIMETRY

The results of the MPT will be compared to results of an established technique; combined Particle Image Velocimetry (PIV) and Digital Image Analysis (DIA)[11,12]. PIV is a non-intrusive optical technique that provides the displacement of particles between two consecutive images of a high-speed camera. For analysis the images are split in interrogation areas, where a cross-correlation function is used to determine the most likely displacement. In this study, interrogation areas of 64x64 pixels are used with 50% overlap. The instantaneous particle velocity is determined from the particle displacement, with M the image magnification in pixels/m:

$$\bar{v}_p(x,t) = \frac{\bar{s}_p(x,t)}{M\Delta t} \qquad (8)$$

Outliers were removed using a median filter. PIV does not account for differences in dense and dilute areas, which would result in averaged particle velocities biased towards dilute areas where high velocities generally occur. To correct for this, Digital Image Analysis (DIA) is used. DIA is able to determine the local solids fraction of a cell.

DIGITAL IMAGE ANALYSIS

The digital image analysis technique used in this work is based on the algorithm of van Buijtenen et al.[12] and de Jong et al.[11]. Given the intensity of the interrogation area, a 2D or apparent particle volume fraction is obtained for each interrogation area. Afterwards

9

a correction for 2D to 3D particle volume fraction is used, following equation 9.

$$\varepsilon_{p,3D} = min\left(0.6, \frac{A\epsilon_{p,2D}}{1 - \frac{1}{B}\epsilon_{p,2D}}\right) \tag{9}$$

Combining the information of the DIA with that of PIV results in a weighted average velocity following equation 10

$$\langle \bar{v}_p \rangle_{i,j} = \frac{\sum_{i,j} \bar{v}_p(x,t)\varepsilon_{p,3D}}{\sum_{i,j} \varepsilon_{p,3D}} \tag{10}$$

This weighted velocity is comparable to the velocity obtained with MPT as it is no longer biased by differences in solids volume fraction.

MPT VALIDATION

From equation 1 it can be seen that the strength of the magnetic field depends mainly on two parameters; the magnetic moment of the marker, which depends on the volume and composition of the magnet, and the distance to the sensor. To test the influence of these two parameters, the error margins and limitations of the MPT were determined for stationary magnets in a 3D setup, as depicted in figure 2. As a second test, a prescribed and simple pendulum motion was applied to the magnet to study the tracking capability of the MPT with the pseudo 2D sensor array. Finally the MPT is compared to the established PIV-DIA technique in a pseudo 2D fluidized bed.

EFFECT OF MAGNETIC MOMENT

To study the effect of the magnetic moment on the performance of the MPT technique, magnets with different sizes and thus magnetic moments where positioned in the centre of the 3D sensor array on top of a platform in between the second and third ring. A schematic representation is given in Figure 5. The properties of the different markers

10

used in this study are given in Table 3. Using the SQP and LM algorithms the spread in data points was determined by looking at the standard deviation of the data positions in x- and y-direction, by sampling the data at 50 Hz. The results are shown in Figure 6, depicting the error of the analysis as a function of the magnetic moment for the different non-linear optimization schemes.

Figure 6 shows a first order dependency of the magnetic field with the magnetic moment, which was expected. It can also be seen that for this most extreme case (largest distance from the sensors), for low magnetic moments near 0.01 Am^2, the error rapidly increases to 10 mm, which would be unsuited for actual experiments in fluidized beds.

To better display the power of the SQP analysis, the scatter of the 0.013 Am^2 marker (no. 2) is shown in Figure 7 for the LM and SQP Algorithms, using the data sampled at 200 Hz. The LM method is less accurate and can reach $\pm \infty$, which happens 3 times. Furthermore 1 % of all LM data falls outside of the physical bounds of the setup. The SQP method is able to contain all position calculations within physical bounds and is a factor 2 more accurate, which is possible by addition of constraints to the optimization function and using a smart filtering. In general the SQP method is better suited to determine the position of a stationary marker.

EFFECT OF DISTANCE TO SENSOR

Similar experiments were performed for two of the markers (no. 4 and 6) with magnetic moment of 0.03 Am^2 and 0.18 Am^2, to study the effect of the relative distance of the magnets with respect to the sensors. The markers were positioned with increasing distance from one of the sensors as depicted in Figure 5. The results are shown in Figure 8. The results for the largest marker are acceptable as only a small decrease in accuracy was found with increasing the relative distance. However, for the smaller marker the error in the analysis of the position increases rapidly to 2.5 mm, when the marker is positioned towards the centre of the setup. This clearly indicates the importance of a proper design of the sensor array combined with a proper choice of marker with respect to the domain

11

of interest.

Furthermore, no radical effects of the orientation were found in the 3D setup; the results follow a similar trend as the particle position. An endurance test for the system was performed and no decrease in performance or signal drift was found for two hours.

SIMPLE PENDULUM MOTION

To study the performance of the MPT as a particle tracking technique, movement of the magnet was induced. In a second test case a magnetic marker was suspended from a thin wire and given a swing. The resultant pendulum motion was compared with a dampened harmonic oscillator function, for the sideways motion (x):

$$x = e^{-\gamma t} a \cos(\omega t - \alpha) \tag{11}$$

The two smallest markers, i.e. with the smallest magnetic moment: $\mu = 0.013$ and $\mu = 0.003$ Am^2, have been used in combination with the 2D sensor array. Note that the pseudo 2D setup and sensor array allow for a short distance between the markers and the sensor array, giving good signal quality, even with small magnetic moments.

The sideways motion of the magnetic marker with $\mu = 0.013$ Am^2 is shown in Figure 9. A very well behaved dampened harmonic motion can be observed and it can be seen that the fit with equation 11 is very good. The marker with $\mu = 0.003$ Am^2 is shown in Figure 10. For comparison results from both the LM and the SQP algorithms are shown. The LM algorithm has trouble to properly locate the marker and sometimes shows some strange peaks at the end of the swing, which is near to the edge of the 2D sensor array. The inability of the LM algorithm can be attributed to the lack of constraints. By adding these constraints via the SQP algorithm the optimization converges to the correct point. This can clearly be seen in Figure 10, where for the SQP algorithm a smooth profile can be seen. The fit is not as good as for the marker with magnetic moment $\mu = 0.013$ Am^2, but still a remarkable fit with the motion of a dampened harmonic oscillator is found.

12

COMPARISON OF MPT WITH PIV-DIA

As a true performance test the MPT was compared to PIV-DIA, a well-established measurement technique. A magnetic marker was fluidized in a pseudo 2D fluidized bed for 1 hour for the MPT and a mere 25 seconds for the PIV-DIA. This results in an average of 5000 data points per interrogation area for PIV-DIA and 230 for MPT. The properties of the magnetic marker and the bed material are given in Table 3. A magnetic marker with $\mu = 0.0125$ Am^2 was chosen as from the pendulum swing we already found that this marker was easy to follow. The minimum fluidization velocity of the bed material is 1.7 m/s, determined with standard pressure drop analysis. The estimated minimum fluidization velocity of the magnetic marker is 1.82 m/s using the Beetstra correlation[15]. To avoid segregation of the magnetic marker, background velocities u_{bg} of 2.5 and 3.5 m/s have been used.

The time-averaged velocity fields of the fluidized beds obtained with the two techniques are shown in figure 11, fluidized with a background velocity of 2.5 m/s. High particle velocities can be found in the centre of the bed, where the bubbles predominately rise. The particle velocities in the annulus are very low. A larger part of the flow seems to come from the right side of the bed, which can be attributed to (minor) maldistribution of the distributor plate. Still the typical circulation patterns are clearly obtained. Overall the results of the MPT and PIV-DIA compare very well.

Figure 12 and 13 show the vertical velocity components obtained from the two techniques at three different heights in the pseudo 2D bed. These results reveal very good agreement between the two techniques. At low velocities some deviations for the MPT can be seen which can be attributed to the larger error margins, which can be expected from the magnetic marker position determination and the lower number of data points per interrogation area.

The large velocities in the centre of bed compare very well however, especially for the experiment with a background velocity of 3.5 m/s.

13

The solids volume fractions were obtained from MPT and DIA as well using equations 7 and 9 respectively. Figure 14 shows the time-averaged solids fraction in the fluidized bed. The dense packing in the annulus can be clearly seen, also the slight maldistribtion of the distributor plate shows again with both techniques. The DIA technique is however much more smooth which is due to the larger amount of data available for averaging. The MPT technique has fewer data points which is reflected in this contour plot.

Figure 15 shows the direct comparison of the solids volume fractions of all interrogation areas. In this parity plot the lack of data points for the MPT shows more clearly. Especially in the dense zone the MPT sometimes has a lower solids volume fraction, the general trend however is quite clear and shows a reasonable agreement between MPT and DIA based results. The results of the MPT in general compares very well to PIV-DIA qualitatively. Quantitatively the particle velocities compare very well, a quantitative description of the solids fraction with MPT is currently not able to match itself with DIA. Possibly with longer measurement time, yielding more data points per interrogation area, this might be countered.

CONCLUSIONS

The newly developed analysis tool for the magnetic particle tracking technique (MPT) using sequential quadratic programming (SQP) and wavelet filtering has been presented and extensively tested. It was shown that the strength of the MPT depends heavily on the magnetic moment (μ) of the marker and the relative distance to the sensor array. Furthermore the newly developed method for data analysis, SQP in combination with wavelet filtering shows a great improvement on the results, owing largely to the addition of physical constraints to the non-linear optimization function.

The results of the magnetic particle tracking technique (MPT) have been compared for a pseudo 2D fluidized bed with a well-established non-invasive measuring technique for granular flow: particle image velocimetry (PIV) and digital image analysis (DIA).

14

The results compare well, showing the strength of the MPT for measuring granular flow behaviour.

Future studies will entail the rotational behaviour of the magnetic markers as well as comparison of the MPT with computational discrete particle modelling (DPM).

Acknowledgements

List of Symbols

Roman symbols

H	Magnetic field	A/m
Q	Quality function	(-)
S	Sensor signal	A/m
e	unit vector	(-)
v	velocity	m/s
s	pixel displacement	pixel
M	Magnification	pixel/m
N	Number of	(-)
t	time	s
A	Fitting parameter	(-)
B	Fitting parameter	(-)

Greek symbols

15

μ	Magnetic moment	Am^2
ε	porosity	(-)

Abbreviations and subscripts

MPT Magnetic Particle Tracking

PIV Particle Image Velocimetry

DIA Digital Image Analysis

SQP Sequential Quadratic Programming

x in the x-direction

y in the y-direction

z in the z-direction

p particle

m measured

t theoretical

References

1 Parker DJ, Leadbeater TW, Fan X, Hausard MN, Ingram A, and Yang Z. Positron imaging techniques for process engineering: recent developments at birmingham. Measurement Science and Technology. 2008, 19(9):094004.

2 Degaleesan S, Dudukovic MP, and Pan Y. Application of wavelet filtering to the radioactive particle tracking technique. Flow measurement and instrumentation. 2002, 13(1):31–43.

3 Chaouki J, Larachi F, and Dudukovic MP. Non-invasive monitoring of multiphase flows. Access Online via Elsevier, 1997.

4 Richert H, Hilgenfeld B, and Görnert P. Magnetic sensor techniques for new intelligent

16

endoscopic capsules. In the Proc. of the 10th Symposium Magnetoresistive Sensors and Magnetic Systems, 2009.

5 Richert H, Kosch O, and Görnert P. Magnetic monitoring as a diagnostic method for investigating motility in the human digestive system. In: Andrä W and Nowak H, ed., Magnetism in Medicine: A Handbook, Second Edition. Wiley-VCH Verlag, 2007, 481–498.

6 Mohs G, Gryczka O, Heinrich S, and Mörl L. Magnetic monitoring of a single particle in a prismatic spouted bed. Chemical Engineering Science. 2009, 64(23):4811–4825.

7 Halow J, Holsopple K, Crawshaw B, Daw S, and Finney C. Observed mixing behavior of single particles in a bubbling fluidized bed of higher-density particles. Industrial & Engineering Chemistry Research. 2012, 51(44):14566–14576.

8 Neuwirth J, Antonyuk S, Heinrich S, and Jacob M. CFD-DEM study and direct measurement of the granular flow in a rotor granulator. Chemical Engineering Science. 2013, 86:151–163.

9 Idakiev V and Mörl L. How to measure the particle translation and rotation in a spouted and fluidized bed. Journal of Chemical Technology & Metallurgy. 2013, 48 (5):445–450.

10 Hu C, Li M, Song S, Zhang R, Meng MQH, et al. A cubic 3-axis magnetic sensor array for wirelessly tracking magnet position and orientation. Sensors Journal, IEEE. 2010, 10(5):903–913.

11 de Jong JF, Odu SO, van Buijtenen MS, Deen NG, van Sint Annaland M, and Kuipers JAM. Development and validation of a novel digital image analysis method for fluidized bed particle image velocimetry. Powder Technology. 2012, 190:193–202.

12 van Buijtenen MS, Börner M, Deen NG, Heinrich S, Antonyuk S, and Kuipers JAM.

17

An experimental study of the effect of collision properties on spout fluidized bed dynamics. Powder Technology. 2011, 206(1):139–148.

13 Nocedal J and Wright SJ. Numerical Optimization, 2nd edition. Springer, 2006.

14 Wildman RD, Huntley JM, Hansen JP, Parker DJ, and Allen DA. Single-particle motion in three-dimensional vibrofluidized granular beds. Physical Review E. 2000, 62(3):3826.

15 Beetstra R, Van der Hoef MA, and Kuipers JAM. Drag force of intermediate reynolds number flow past mono-and bidisperse arrays of spheres. AIChE Journal. 2007, 53 (2):489–501.

18

List of Figures

19

List of Tables

20

Figure 1: Magnetic Particle Tracking sensor array (left) and schematic overview of the PIV-DIA setup (right).

21

Figure 2: 3D sensor array, 24 tri-axis AMR sensors in 4x6 cylindrical configuration, connected to a controller box(not on the photo.)

22
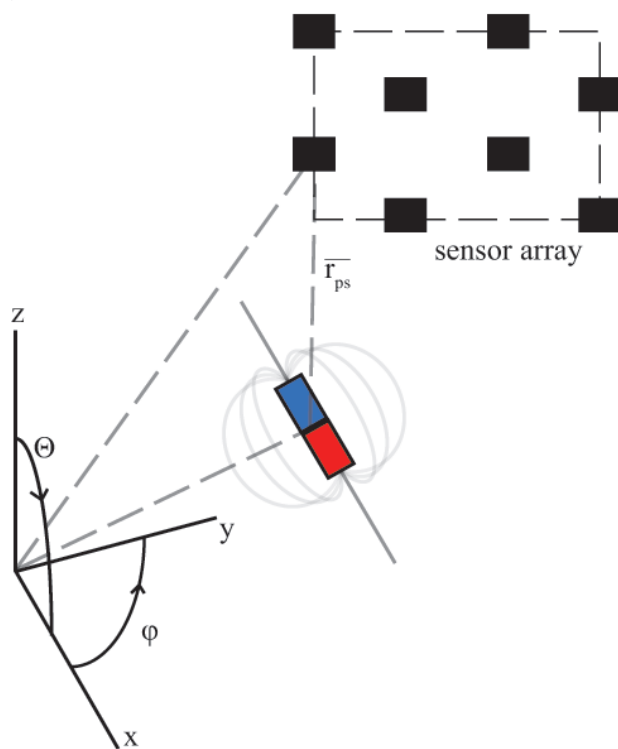
Figure 3: Schematic representation of the principle behind magnetic particle tracking.
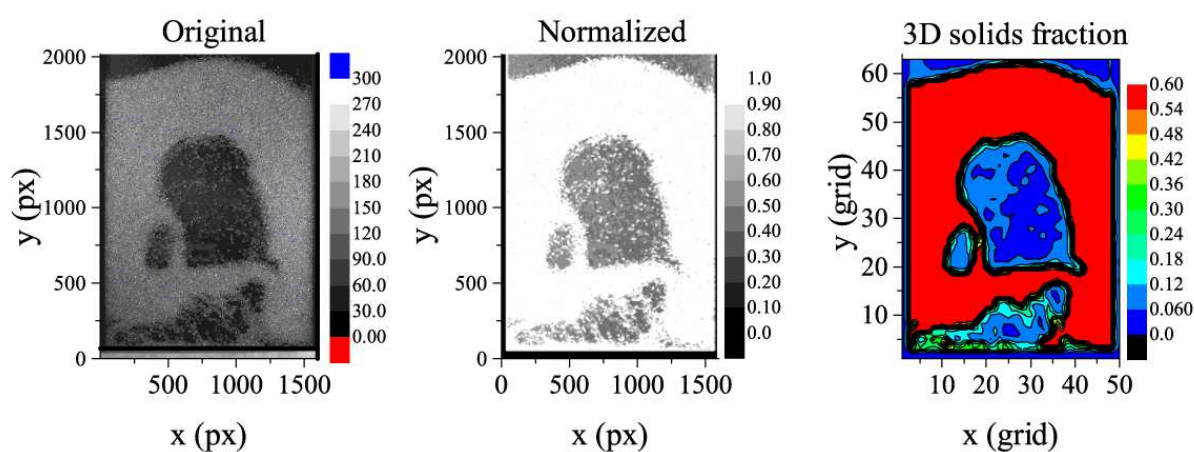
23

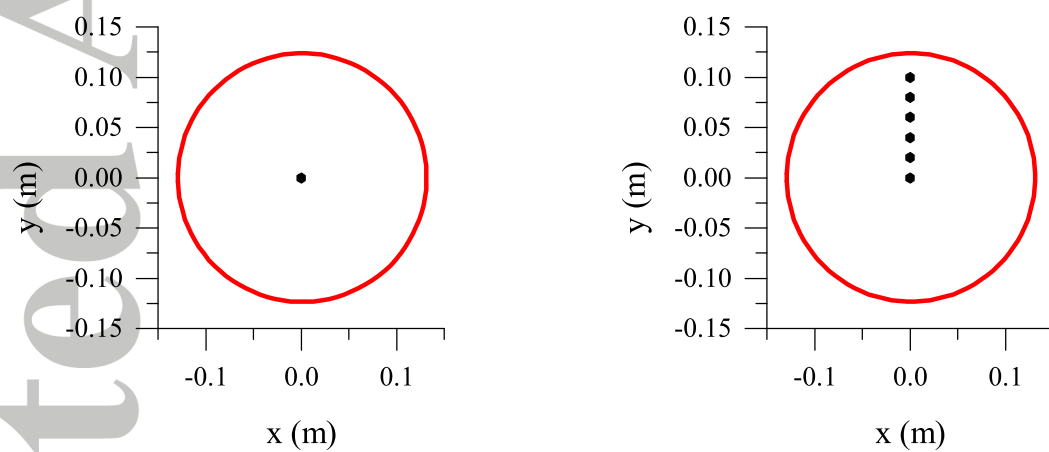Figure 4: Overview of the digital image analysis technique.

24

Figure 5: Schematic overview of the marker positions in the stationary tests (top view). Left; μ dependency. Right; r dependency.
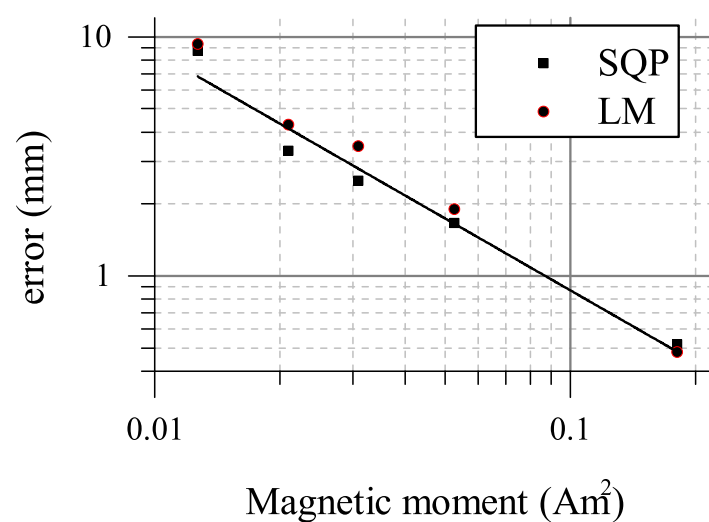
Figure 6: Error dependency of magnetic markers with varying magnetic moment. using the Levenberg Marquardt Algorithm and the Sequential Quadratic Programming algorithm. Linear fit with slope -1.
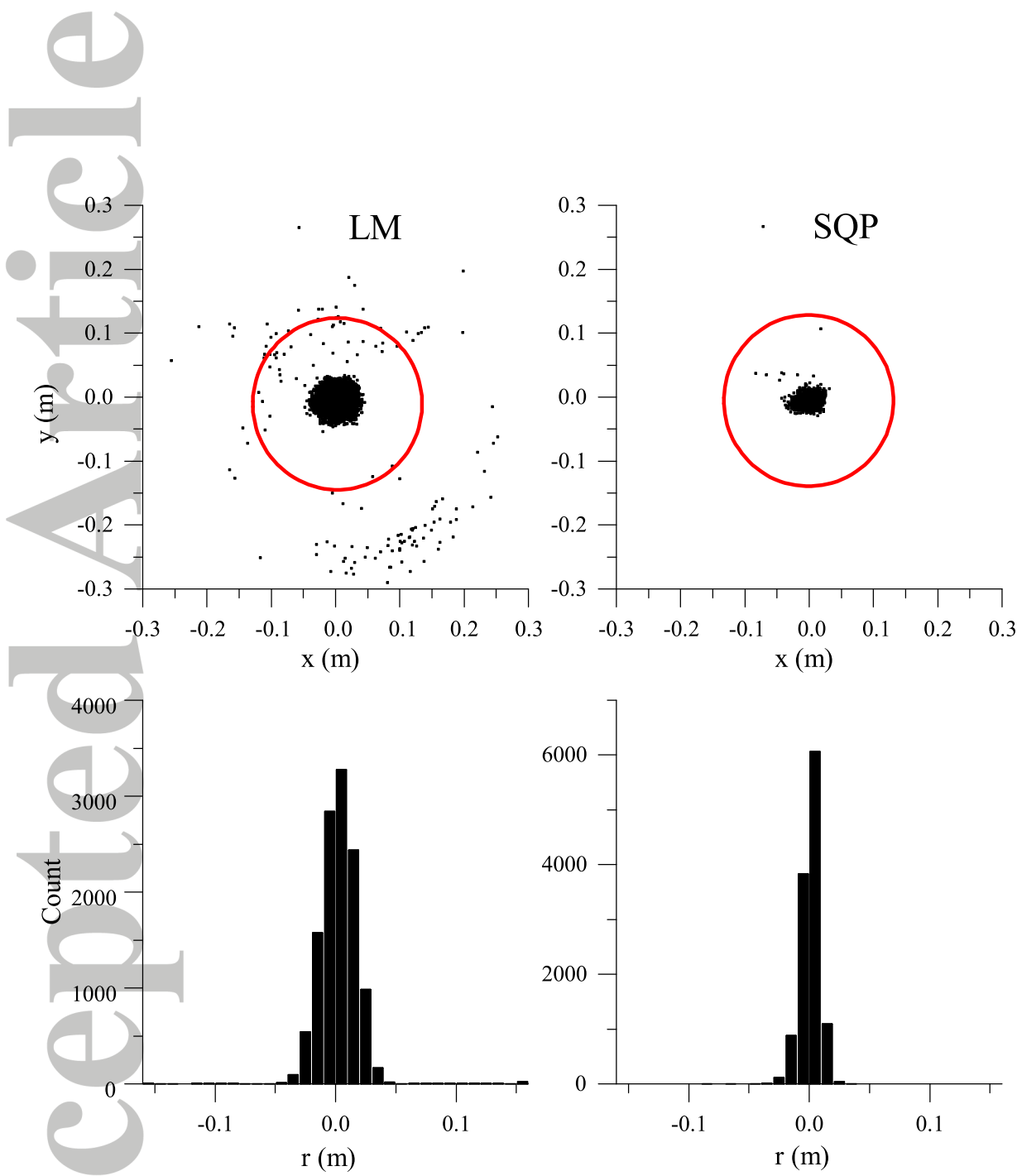
26

Figure 7: Scatter of x,y-positions for LM and SQP algorithms at 200 Hz sampling (top), where the red circle indicates the radial position of the sensors, and histograms of the found locations with respect to the centre of the setup (bottom).
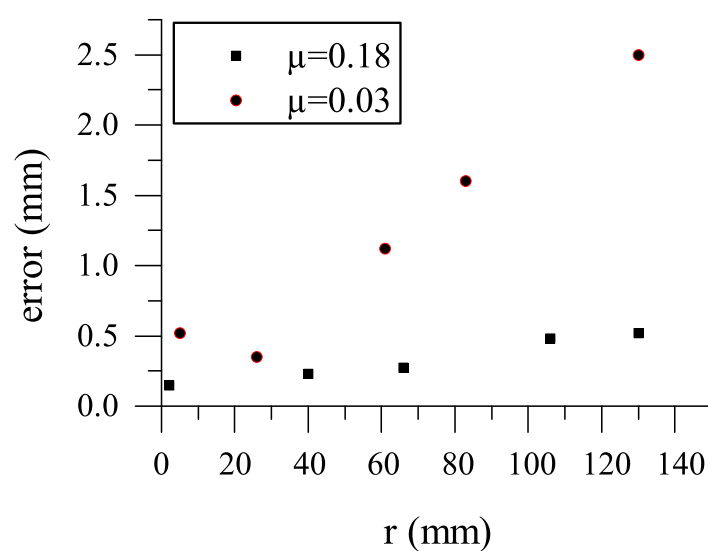
27

Figure 8: Error dependency of two magnetic markers at increasing distance from the nearest sensor using the SQP algorithm. spheres; μ=0.03 Am^2, squares; μ=0.18 Am^2.
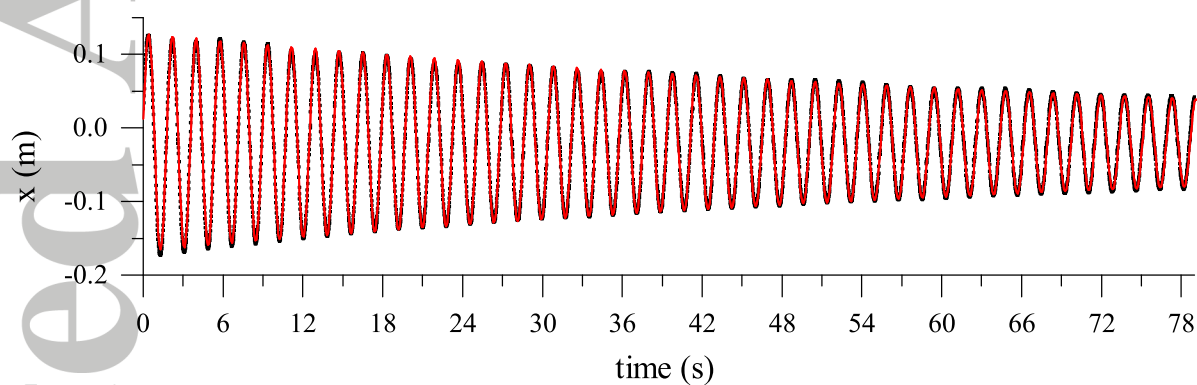
28

Figure 9: Results of the pendulum swing with a marker with a magnetic moment of 0.013 Am^2, using SQP analyis. Fitted with a dampened harmonic oscillator, equation (3.10), with R2=99.7 %.
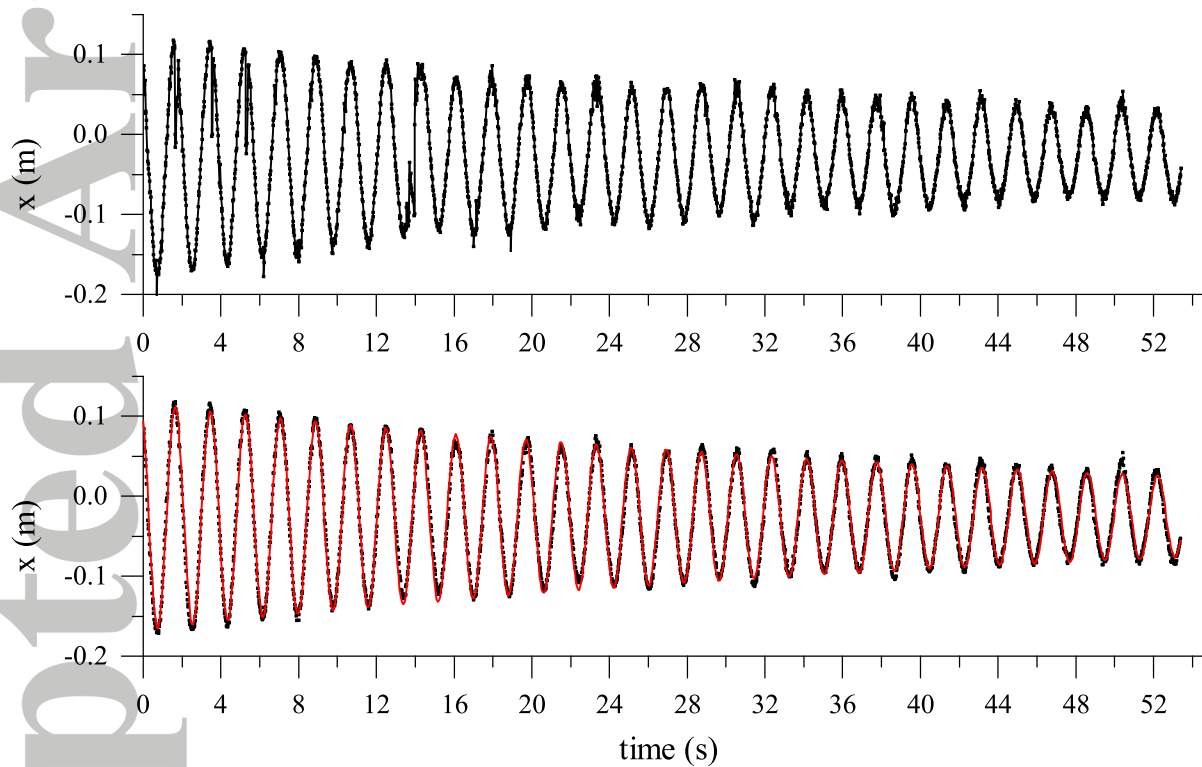
29

Figure 10: Results of the pendulum swing with a marker with a magnetic moment of 0.003 Am^2, using LM analysis; top, and SQP analysis bottom, fitted with a dampened harmonic oscillator, equation (3.10), with R2=98.5 %.
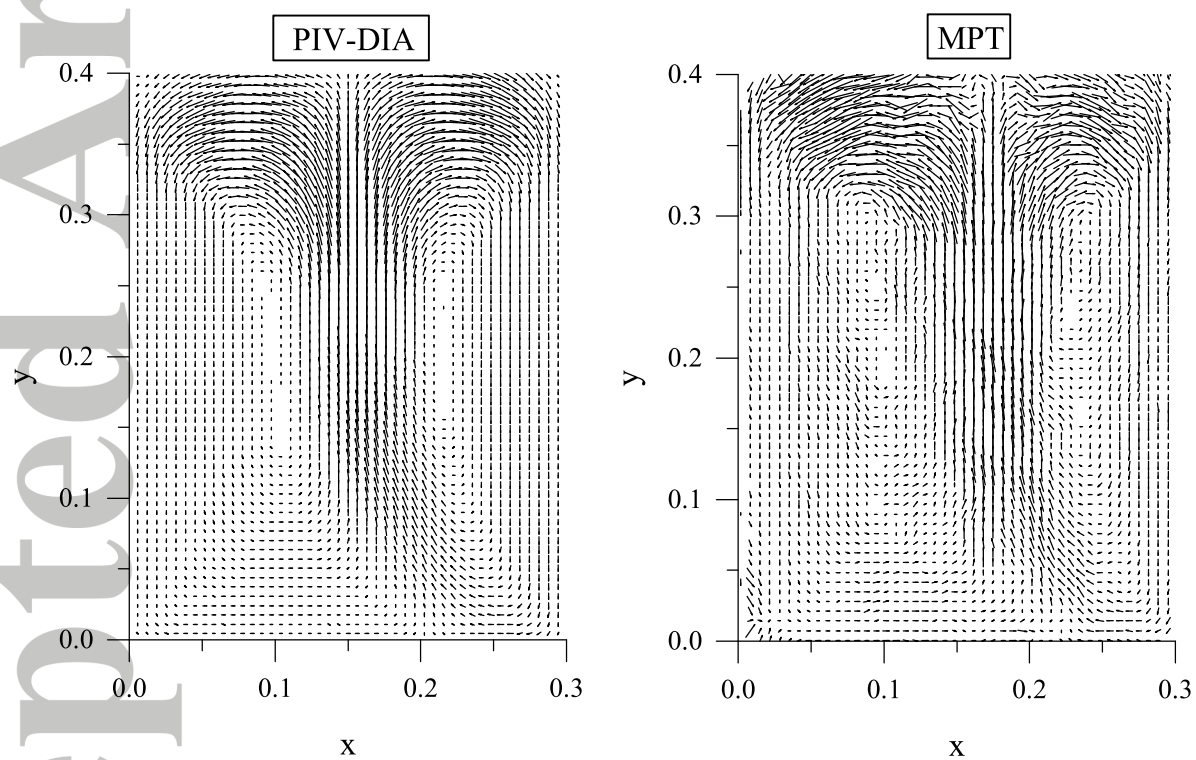
30

Figure 11: Vectorplots of the particle velocity in the pseudo 2D fluidized bed, left; PIV-DIA, right; MPT, $u_{bg} = 2.5$ m/s.
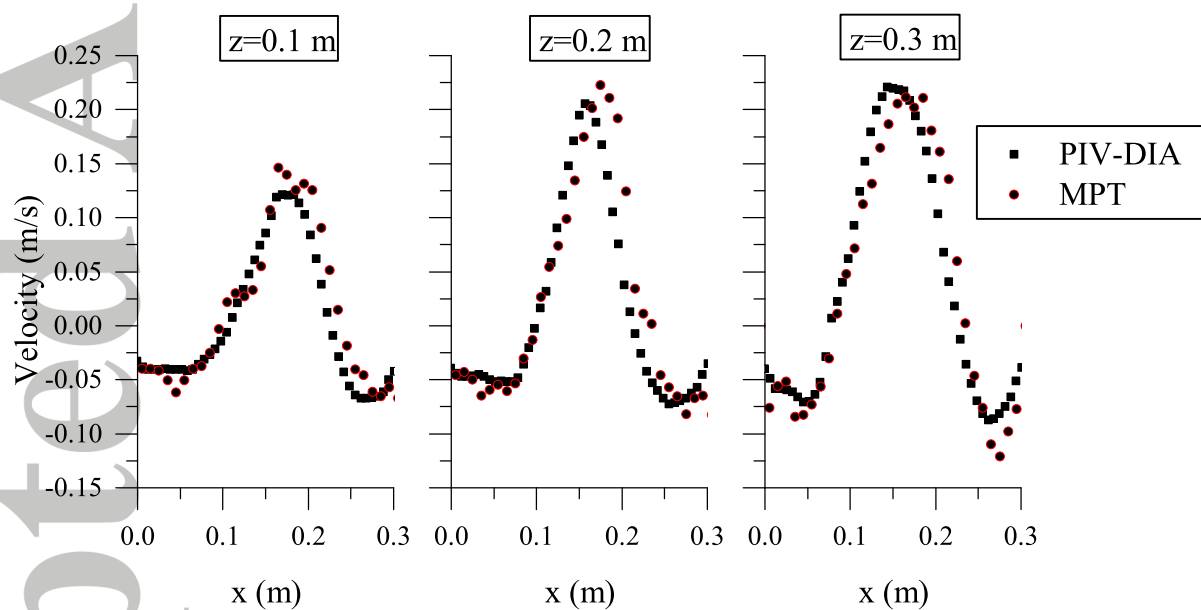
31

Figure 12: Comparison of averaged particle velocity for PIV and MPT in vertical direction at three cross-sections of the bed. $u_{bg} = 2.5$ m/s.
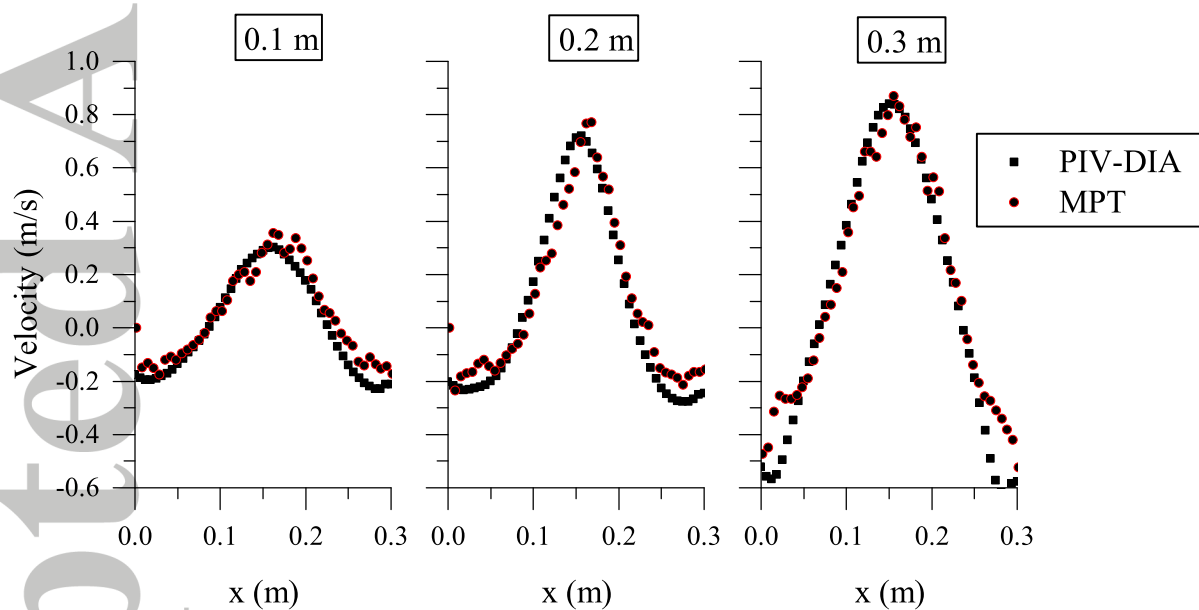
32

Figure 13: Comparison of averaged particle velocity for PIV and MPT in vertical direction at three cross-sections of the bed. $u_{bg} = 3.5$ m/s

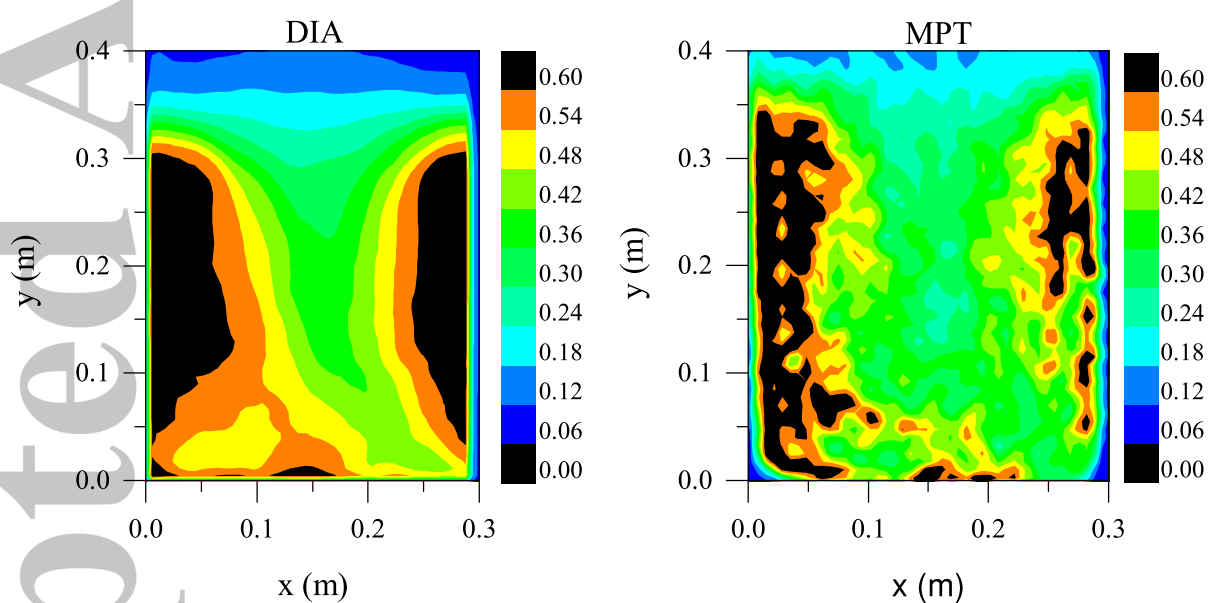Figure 14: Contour plots of the solids volume fraction in the pseudo 2D fluidized bed, left; PIV-DIA, right; MPT, $u_{bg} = 2.5$ m/s .

34

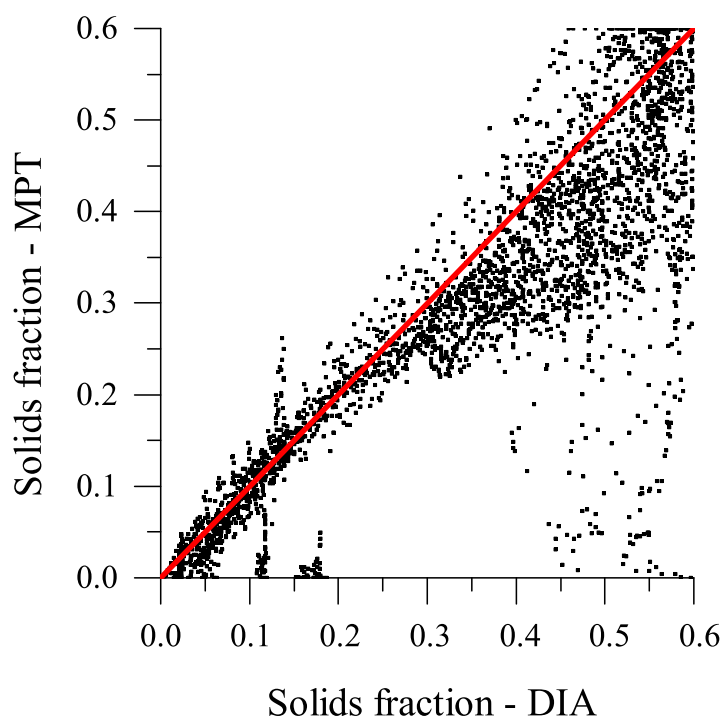Figure 15: Parity plot of the solids fractions obtained with MPT and DIA. $u_{bg} = 2.5$ m/s

Table 1: qualitative comparison of particle tracking techniques

Property	PTV	CARPT/RPT/PEPT	MPT
Costs	$++$	$--$	$++$
Safety measures	$+$	$--$	$+$
Spatial resolution	$+$	$+$	$-$
Geometry & size setup	$-$	$++$	$+$
Spatial resolution	$+$	$+$	$-$

36

Table 2: Settings and Parameters

Fluidized Bed	
Width	0.3 m
Height	1.0 m
Depth	0.015 m
Porous plate	3 mm thick
Average pore size	10 μm
Mass flow controller (max capacity)	1200 l/min
Material front plate	glass
Other materials	alumina & stainless steel (non-magnetic)
High speed camera	LaVision HSG3
Effective resolution	1500 by 2000 pixels
Exposure time	200 μs
Inter-frame time	2 ms
Interogation size (multipass)	128 by 128/64 by 64
MPT sensor array	
Sensor type	tri-axis AMR
Amount	3 * 24
Frequency	1000 Hz
dimensions	0.35, 0.65 m (width, height)
Particles	
Bed material size	2.8-3.2 mm
Density	2526 kg/m^3
Minimum fluidization velocity	1.7 m/s
Magnetic marker size	4.7 mm
Density	2100 kg/m^3
Magnetic moment	0.0125 Am^2
Minimum fluidization velocity	1.8 m/s

37

Table 3: Properties of magnetic markers

No.	Magnet shape	Magnet diameter mm	Particle diameter mm	Particle density kg/m^3	Magnetic moment Am^2
1	sphere	2	3	3300	0.003
2	sphere	3	3.5	4950	0.013
3	sphere	3.5	4.8	2900	0.021
4	sphere	4	4	7400	0.03
5	cylinder	2	10.2	1500	0.05
6	cylinder	2	12	1550	0.18

38